

POLARIZATION PUZZLE IN $B \rightarrow \phi K^*$ AND OTHER $B \rightarrow VV$ AT BABAR

A. GRITSAN

LBNL, 1 Cyclotron Rd., M.S. 50A-2160, Berkeley, CA 94720, USA

E-mail: AVGritsan@lbl.gov

With a sample of about 227 million $B\bar{B}$ pairs recorded with the BABAR detector we perform a full angular analysis of the decay $B^0 \rightarrow \phi K^{*0}(892)$. Ten measurements include polarization, phases, and five CP asymmetries. We also observe the decay $B^0 \rightarrow \phi K^{*0}(1430)$. Polarization measurements are performed with the $B \rightarrow \rho K^*(892)$, $B \rightarrow \rho\rho$, and $B \rightarrow \rho\omega$ decay modes, and limits are set on the $B \rightarrow \omega K^*(892)$ decay rates. These measurements help to understand the puzzle of large fraction of transverse polarization observed in $B \rightarrow \phi K^*$ decays and allow for new ways to study CP violation and potential new amplitude contributions.

1 Introduction

The decay $B \rightarrow \phi K^*(892)$ is expected to have contributions from $b \rightarrow s$ loop penguin transitions while the tree-level transition is suppressed in the Standard Model. Angular correlation measurements and asymmetries are particularly sensitive to amplitudes arising outside the Standard Model¹. The first evidence for this decay was provided by the CLEO² and BABAR³ experiments. The large fraction of transverse polarization observed by BABAR⁴ and confirmed by BELLE⁵ was a surprise and enabled a full angular analysis described by ten parameters for contributing amplitudes and their phases.

Similarly, the decays $B \rightarrow \rho K^*(892)$ and $B \rightarrow \omega K^*(892)$ are expected to have contributions from $b \rightarrow s$ loop transitions with some tree contributions. Polarization measurements in these channels may help in understanding the $B \rightarrow \phi K^*$ polarization puzzle. The decays $B \rightarrow \rho\rho$ and $\omega\rho$ are expected to proceed through the tree-level $b \rightarrow u$ transition and through CKM-suppressed $b \rightarrow d$ penguin transitions. These are particularly interesting modes for the CKM angle α studies and have the advantage of a larger decay rate and smaller uncertainty in penguin pollution compared to $B \rightarrow \pi\pi$. The BABAR^{4,6} and the BELLE⁷ experiments reported observation of the $B \rightarrow \rho K^*$ and $\rho\rho$ decays.

The angular distribution of the $B \rightarrow VV$

decay products are expressed as a function of $\cos\theta_i$ and Φ , where θ_i is the helicity angle of a ϕ , K^* , ρ , or ω , and Φ is the angle between the two resonance decay planes. The differential decay width has three complex amplitudes A_λ corresponding to the vector meson helicity $\lambda = 0$ or ± 1 ^{1,8}. The last two can be expressed in terms of $A_{\parallel} = (A_{+1} + A_{-1})/\sqrt{2}$ and $A_{\perp} = (A_{+1} - A_{-1})/\sqrt{2}$.

In this paper we present the latest results from BABAR in a number of charmless $B \rightarrow VV$ decays. We measure the branching fraction, the polarization parameters $f_L = |A_0|^2/\Sigma|A_\lambda|^2$, $f_{\perp} = |A_{\perp}|^2/\Sigma|A_\lambda|^2$, and the relative phases $\phi_{\parallel} = \arg(A_{\parallel}/A_0)$, $\phi_{\perp} = \arg(A_{\perp}/A_0)$. We allow for CP -violating differences between the \bar{B}^0 ($Q = +1$) and B^0 ($Q = -1$) decay amplitudes (\bar{A}_λ and A_λ), and derive vector triple-product asymmetries¹:

$$A_T^{\parallel,0} = \frac{1}{2} \left(\frac{\text{Im}(A_{\perp} A_{\parallel,0}^*)}{\Sigma|A_\lambda|^2} + \frac{\text{Im}(\bar{A}_{\perp} \bar{A}_{\parallel,0}^*)}{\Sigma|\bar{A}_\lambda|^2} \right)$$

The B flavor sign Q can be determined in the self-tagging final state, then we have ten independent measured quantities:

$$\begin{aligned} n_{\text{sig}}^Q &= n_{\text{sig}} (1 + Q \mathcal{A}_{CP})/2; \\ f_L^Q &= f_L (1 + Q \mathcal{A}_{CP}^0); \\ f_{\perp}^Q &= f_{\perp} (1 + Q \mathcal{A}_{CP}^{\perp}); \\ \phi_{\parallel}^Q &= \phi_{\parallel} + Q \Delta\phi_{\parallel}; \\ \phi_{\perp}^Q &= \phi_{\perp} + \frac{\pi}{2} + Q (\Delta\phi_{\perp} + \frac{\pi}{2}). \end{aligned}$$

Work supported in part by the Department of Energy, contract DE-AC02-76SF00515

Stanford Linear Accelerator Center, Stanford University, Stanford, CA 94309

Experimental technique

We use data collected with the *BABAR* detector⁹ at the PEP-II asymmetric-energy e^+e^- collider operated at the center-of-mass energy of the $\Upsilon(4S)$ resonance ($\sqrt{s} = 10.58$ GeV). We fully reconstruct vector-vector B meson decays involving ϕ , ρ , ω , and K^* resonances. We identify B meson candidates using two variables: $m_{ES} = [(s/2 + \mathbf{p}_i \cdot \mathbf{p}_B)^2/E_i^2 - \mathbf{p}_B^2]^{1/2}$ and $\Delta E = (E_i E_B - \mathbf{p}_i \cdot \mathbf{p}_B - s/2)/\sqrt{s}$, where (E_i, \mathbf{p}_i) is the initial state four-momentum, and (E_B, \mathbf{p}_B) is the four-momentum of the reconstructed B candidate. To reject the dominant quark-antiquark continuum background we apply event-shape requirements.

We use an unbinned maximum-likelihood (ML) fit to extract signal parameters. There are several event categories j : signal, continuum $q\bar{q}$, combinatoric $B\bar{B}$ background, and specific B -decay background modes. The likelihood for each candidate i is defined as $\mathcal{L}_i = \sum_{j,k} n_j^k \mathcal{P}_j^k(\vec{x}_i; \vec{\alpha}; \vec{\beta})$, where each of the $\mathcal{P}_j^k(\vec{x}_i; \vec{\alpha}; \vec{\beta})$ is the probability density function for input variables. The n_j^k is the number of events with the B flavor k in the category j . The event yields n_j , asymmetries \mathcal{A}_j , and the signal polarization parameters $\vec{\alpha}$ are obtained by maximizing $\mathcal{L} = \exp(-\sum n_j^k) \prod \mathcal{L}_i$.

In Fig. 1 examples of fit input variables and ML fit projections are shown, where data

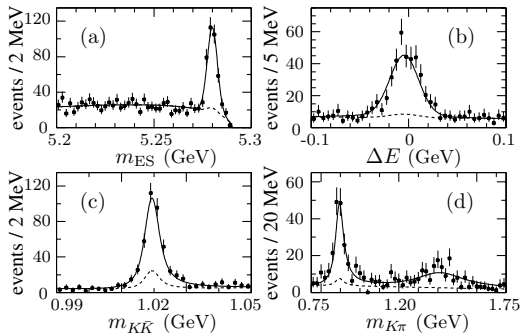


Figure 1. Projections onto the variables m_{ES} (a), ΔE (b), $m_{K\bar{K}}$ (c), and $m_{K\pi}$ (d) for the signal $B^0 \rightarrow \phi K^{*0}(892)$ and $\phi K^{*0}(1430)$ candidates combined.

distributions are shown with the signal enhanced with a requirement on the signal-to-background probability ratio calculated with the plotted variable excluded.

Results

The results of our maximum likelihood fit to the sample of $B^0 \rightarrow \phi K^{*0}(892)$ candidates are summarized in Table 1. We observe, with more than 5σ significance, non-zero contributions from all of the three amplitudes A_0 , A_\perp , and A_\parallel ($f_L + f_\perp + f_\parallel = 1$). We find 3σ evidence for non-zero final-state-interaction phases (ϕ_\parallel and ϕ_\perp differ from π or zero). We also observe $B^0 \rightarrow \phi K^{*0}(1430)$ decays.

In Table 2 we show results for all $B \rightarrow VV$ modes with the dominant $b \rightarrow s$ penguin contribution expected. Naive SU(3) decomposition of the relative penguin and tree dia-

Table 1. Summary of the $B^0 \rightarrow \phi K^{*0}(892)$ fit results. We show results for the ten primary signal fit parameters and the derived branching fraction \mathcal{B} and triple-product asymmetries \mathcal{A}_T^\parallel and \mathcal{A}_T^0 .

Fit parameter	Fit result
n_{sig} (events)	$201 \pm 20 \pm 6$
f_L	$0.52 \pm 0.05 \pm 0.02$
f_\perp	$0.22 \pm 0.05 \pm 0.02$
ϕ_\parallel (rad)	$2.34_{-0.20}^{+0.23} \pm 0.05$
ϕ_\perp (rad)	$2.47 \pm 0.25 \pm 0.05$
\mathcal{A}_{CP}	$-0.01 \pm 0.09 \pm 0.02$
\mathcal{A}_{CP}^0	$-0.06 \pm 0.10 \pm 0.01$
\mathcal{A}_{CP}^\perp	$-0.10 \pm 0.24 \pm 0.05$
$\Delta\phi_\parallel$ (rad)	$0.27_{-0.23}^{+0.20} \pm 0.05$
$\Delta\phi_\perp$ (rad)	$0.36 \pm 0.25 \pm 0.05$
\mathcal{B}	$(9.2 \pm 0.9 \pm 0.5) \times 10^{-6}$
\mathcal{A}_T^\parallel	$-0.02 \pm 0.04 \pm 0.01$
\mathcal{A}_T^0	$+0.11 \pm 0.05 \pm 0.01$

Table 2. The *BABAR* measurements of the branching fractions (\mathcal{B}) and polarizations (f_L) of the $B \rightarrow VV$ decays with the dominant $b \rightarrow s$ penguin contribution. Relative coefficients in front of the penguin, color-allowed and color-suppressed tree amplitudes contributing to each decay mode are shown with α_P , α_T , and α_C . Naive SU(3) decomposition is used for illustration. The last column indicates the number of $B\bar{B}$ pairs used in each analysis. New preliminary results this year are indicated by “new”, while references are given to the published results. The last error in the $\rho^+ K^{*0}$ channel has non-resonant decay rate uncertainty separated.

B decay	α_P	α_T	α_C	$\mathcal{B}(10^{-6})$	f_L	$N_{B\bar{B}}(10^6)$
ϕK^{*0}	$\sqrt{2}$	0	0	$9.2 \pm 0.9 \pm 0.5$	$0.52 \pm 0.05 \pm 0.02$	227 (new)
ϕK^{*+}	$\sqrt{2}$	0	0	$12.7^{+2.2}_{-2.0} \pm 1.1$	$0.46 \pm 0.12 \pm 0.03$	89 (publ. ⁴)
$\rho^0 K^{*0}$	1	0	-1	–	–	–
$\rho^0 K^{*+}$	-1	-1	-1	$10.6^{+3.0}_{-2.6} \pm 2.4$	$0.96^{+0.04}_{-0.15} \pm 0.04$	89 (publ. ⁴)
$\rho^+ K^{*0}$	$\sqrt{2}$	0	0	$17.0 \pm 2.9 \pm 2.0^{+0.0}_{-1.9}$	$0.79 \pm 0.08 \pm 0.04 \pm 0.02$	89 (new)
$\rho^- K^{*+}$	$-\sqrt{2}$	$-\sqrt{2}$	0	< 24 (90% C.L.)	–	123 (new)
ωK^{*0}	1	0	1	< 6.1 (90% C.L.)	–	89 (new)
ωK^{*+}	1	1	1	< 7.4 (90% C.L.)	–	89 (new)

Table 3. The *BABAR* measurements of the branching fractions (\mathcal{B}) and polarizations (f_L) of the $B \rightarrow VV$ decays with the $b \rightarrow u$ tree and $b \rightarrow d$ penguin contributions. Relative coefficients in front of the color-allowed tree, color-suppressed tree, and penguin amplitudes are shown with α_T , α_C , and α_P .

B decay	α_T	α_C	α_P	$\mathcal{B}(10^{-6})$	f_L	$N_{B\bar{B}}(10^6)$
$\rho^- \rho^+$	$\sqrt{2}$	0	$\sqrt{2}$	$30 \pm 4 \pm 5$	$0.99 \pm 0.03^{+0.04}_{-0.03}$	89 (publ. ⁶)
$\rho^0 \rho^+$	1	1	0	$23^{+6}_{-5} \pm 6$	$0.97^{+0.03}_{-0.07} \pm 0.04$	89 (publ. ⁴)
$\rho^0 \rho^0$	0	1	-1	< 1.1 (90% C.L.)	–	227 (new)
$\omega \rho^+$	-1	-1	2	$12.6^{+3.7}_{-3.3} \pm 1.8$	$0.88^{+0.12}_{-0.15} \pm 0.03$	89 (new)
$\omega \rho^0$	0	0	$-\sqrt{2}$	< 3.3 (90% C.L.)	–	89 (new)
$\phi \phi$	0	0	0	< 1.5 (90% C.L.)	–	89 (new)

grams is shown. Transverse polarization fraction in both $B \rightarrow \phi K^*$ (892) charge modes are close to 50%, while this effect is less pronounced in the $B \rightarrow \rho K^*$ (892) modes. At the same time, polarization measurements in the tree-dominated modes presented in Table 3 favor longitudinal polarization dominance.

For B decays to light charmless particles we expect the hierarchy of decay amplitudes to be $|A_0| \gg |A_{+1}| \gg |A_{-1}|$ under the assumption of either loop or tree diagram contribution ¹⁰. Our measurements with the decay $B^0 \rightarrow \phi K^{*0}$ (892) do not agree with the first inequality but agree with the second one. This suggests other contributions to the decay amplitude, previously neglected, either

within or beyond the Standard Model ^{1,11}.

We also observe the decays $B^0 \rightarrow \phi K^{*0}$ (1430) which we find to be predominantly longitudinally polarized based on the ϕ helicity angle distribution. The width and the angular distribution of the K^{*0} (1430) resonance structure are not consistent with the pure K_2^{*0} (1430) tensor state at more than 10σ . However, the angular distribution provides evidence of the longitudinally polarized tensor K_2^{*0} (1430) contribution (with statistical significance of 3.2σ) in addition to the scalar K_0^{*0} (1430). If the longitudinal polarization dominance holds for the vector-tensor $B \rightarrow \phi K_2^*$ (1430) decays, this will point to the special role of the vector current in the

$B \rightarrow \phi K^*(892)$ polarization puzzle.

If one loop diagram dominates the $B \rightarrow \phi K^*$ decay amplitude, the direct CP asymmetries \mathcal{A}_{CP} , \mathcal{A}_{CP}^0 , and \mathcal{A}_{CP}^\perp , and the weak-phase differences $\Delta\phi_{\parallel}$ and $\Delta\phi_{\perp}$, or alternatively \mathcal{A}_T^0 and $\mathcal{A}_T^{\parallel}$, are expected to be negligible. These are interesting to look for new amplitude contributions with different weak phases.

The rates of the $B^0 \rightarrow \rho^+ \rho^-$ and $B^+ \rightarrow \rho^0 \rho^+$ decays are larger than the corresponding rates of $B \rightarrow \pi\pi$ decays¹². At the same time, the measurements of the $B \rightarrow \rho K^*$ branching fractions do not show significant enhancement with respect to $B \rightarrow \pi K$ decays¹², both of which are expected to be dominated by $b \rightarrow s$ penguin diagrams. We can use flavor $SU(3)$ to relate $b \rightarrow s$ and $b \rightarrow d$ penguins; the measured branching fractions indicate that the relative penguin contributions in the $B \rightarrow \rho\rho$ decays are smaller than in the $B \rightarrow \pi\pi$ case.

A more quantitative estimate of penguin contributions in $B \rightarrow \rho\rho$ decays can be obtained using isospin relations and measurements of $B \rightarrow \rho^0 \rho^0$, $\rho^+ \rho^-$, and $\rho^+ \rho^0$ branching fractions and polarization^{6,13}. Since the tree contribution to the $B^0 \rightarrow \rho^0 \rho^0$ decay is color-suppressed (see Table 3), the decay rate is sensitive to the penguin diagram and its tight experimental limit provides tight constraints on penguin pollution. This makes $B^0 \rightarrow \rho^+ \rho^-$ an ideal channel for the time-dependent measurement of the CKM angle α . It is interesting to note that $B^0 \rightarrow \omega \rho^0$ measurement provides comparable constraint on penguin contribution, but additional assumptions are required.

Acknowledgments

I am grateful for the excellent work by *BABAR* members who contributed results and made this work possible. I would like to thank Bob Cahn, Alex Kagan, Zoltan Ligeti, David London, Jim Smith, Mahiko Suzuki, and Arkady

Vainshtein for useful discussions.

References

1. G. Valencia, Phys. Rev. D **39**, 3339 (1989); A. Datta and D. London, Int. J. Mod. Phys. A **19**, 2505 (2004).
2. CLEO Collaboration, R.A. Briere *et al.*, Phys. Rev. Lett. **86**, 3718 (2001).
3. *BABAR* Collaboration, B. Aubert *et al.*, Phys. Rev. Lett. **87**, 151801 (2001); Phys. Rev. D **65**, 051101 (2002).
4. *BABAR* Collaboration, B. Aubert *et al.*, Phys. Rev. Lett. **91**, 171802 (2003); hep-ex/0303020.
5. BELLE Collaboration, K.-F. Chen *et al.*, Phys. Rev. Lett. **91**, 201801 (2003).
6. *BABAR* Collaboration, B. Aubert *et al.*, Phys. Rev. D **69**, 031102 (2004); hep-ex/0404029, submitted to Phys. Rev. Lett.
7. BELLE Collaboration, J. Zhang *et al.*, Phys. Rev. Lett. **91**, 221801 (2003).
8. G. Kramer and W.F. Palmer, Phys. Rev. D **45**, 193 (1992); H.-Y. Cheng and K.-C. Yang, Phys. Lett. B **511**, 40 (2001); C.-H. Chen, Y.-Y. Keum, and H.-n. Li, Phys. Rev. D **66**, 054013 (2002).
9. *BABAR* Collaboration, B. Aubert *et al.*, Nucl. Instrum. Methods **A479**, 1 (2002).
10. A. Ali *et al.*, Z. Phys. C **1**, 269 (1979); M. Suzuki, Phys. Rev. D **66**, 054018 (2002).
11. Y. Grossman, Int. J. Mod. Phys. A **19**, 907 (2004), A. Kagan, hep-ph/0405134; P. Colangelo, F. De Fazio, and T.N. Pham, hep-ph/0406162; W.-S. Hou and M. Nagashima, hep-ph/0408007.
12. Particle Data Group, S. Eidelman *et al.*, Phys. Lett. **B592**, 1 (2004).
13. M. Gronau and D. London, Phys. Rev. Lett. **65**, 3381 (1990); Y. Grossman and H. Quinn, Phys. Rev. D **58**, 017504 (1998); A.F. Falk *et al.*, Phys. Rev. D **69**, 011502 (2004).